Simulation of Variation Potential in Higher Plant Cells

**Vladimir Sukhov · Elena Akinchits ·
Lyubov Katicheva · Vladimir Vodeneev**

Variation potential (VP), a propagating electrical signal unique to plants, induces a number of changes in many physiological processes. However, the mechanisms of its generation and propagation are still under discussion and require experimental and theoretical analysis, including VP simulations. The mathematical model for VP formation in plants has been worked out and is based on our previous description of electrophysiological processes in higher plant cells, including plasma membrane ion transport systems (K^+, Cl^- and Ca^{2+} channels, H^+ and Ca^{2+}-ATPase, $2H^+/Cl^-$ symporter and H^+/K^+ antiporter) and their regulation, ion concentration changes in cells and extracellular spaces and buffers in cytoplasm and apoplast. In addition, the VP model takes into account wound substance diffusion, which is described by a one-dimensional diffusion equation, and ligand-gated Ca^{2+} channels, which are activated by this substance. The VP model simulates the experimental dependence of amplitude, velocity and shape of VP on the distance from the wounding site and describes the influence of metabolic inhibitors, divalent cation chelators and anion channel blockers on the generation of this electrical reaction, as shown in experiments. Thus, our model favorably simulates VP in plants and theoretically supports the role of wound substance diffusion and Ca^{2+} influx in VP development.

Keywords Variation potential · Higher plant ·
Mathematical model · Ion channel · H^+-ATPase ·
Wound substance diffusion

V. Sukhov (✉) · E. Akinchits · L. Katicheva · V. Vodeneev
Department of Biophysics, State University of Nizhni Novgorod,
Nizhni Novgorod Gagarins Avenue 23, 603950 Nizhny
Novgorod, Russia
e-mail: vssuh@mail.ru

Introduction

Variation potential (VP) is an electrical signal unique to plants (Stahlberg et al. 2006) and considered one of the mechanisms for plant systemic responses to local wounding. VPs have been widely shown in higher plants (Stahlberg et al. 2006; Julien et al. 1991; Stahlberg and Cosgrove 1992; Mancuso 1999), but *Chara* algae can produce similar electrical reactions, as a "death message" (Shimmen 2002). It is known that VP propagation can induce changes in gene expression (Stanković and Davies 1996; Fisahn et al. 2004), production of ethylene and abscisic and jasmonic acids (Dziubinska et al. 2003; Fisahn et al. 2004; Hlaváčková et al. 2006), respiration rate increases (Filek and Koscielniak 1997) and transient decreases in photosynthesis (Koziolek et al. 2003; Lautner et al. 2005; Hlaváčková et al. 2006; Grams et al. 2007, 2009; Sukhov et al. 2012).

VP is a transient membrane depolarization similar to the more commonly known action potential (AP). However, VP is characterized by a slow repolarization phase, variability of shape and amplitude and propagation velocity decreases with increasing distance from the wound zone (Davies 2006; Stahlberg et al. 2006; Fromm and Lautner 2007; Vodeneev et al. 2011, 2012). Thus, the mechanisms of VP generation and propagation are considered to be distinguished from those of AP and are still under discussion.

VP generation is considered to be connected with a transient inactivation of plasma membrane H^+-ATPase, a conclusion supported by observed reduced depolarization with addition of metabolic inhibitors (Julien et al. 1991; Stahlberg and Cosgrove 1992) and by absence of measurable changes in the cell-input resistance at VP formation (Stahlberg and Cosgrove 1992, 1996). However, it is

possible that the VP generation mechanism has a complex nature and includes ionic channel activations (Stahlberg et al. 2006; Vodeneev et al. 2011). In particular, VP generation depends on Ca^{2+} influx (Julien et al. 1991; Vodeneev et al. 2011), whereas calcium ions have been shown to activate Cl^- channels and to decrease H^+-ATPase activity (Lewis et al. 1997; De Nisi et al. 1999; Berestovsky and Kataev 2005; Vodeneev et al. 2006).

The mechanism by which VP propagates through the shoots of higher plants is also uncertain. There are two possible means for VP propagation. The first means relates to hydraulic waves, transmitted from the wound zone, which cause an electrical response in plant cells (Malone and Stankovic 1991; Stahlberg and Cosgrove 1992; Mancuso 1999). This hypothesis is supported by reversible changes in leaf or stem thickness that reflect the propagation of a high-pressure wave (Malone and Stankovic 1991; Stahlberg and Cosgrove 1992; Mancuso 1999) and induction of electrical reactions under the pressure step (Stahlberg and Cosgrove 1997; Stahlberg et al. 2006). However, the speed of hydraulic signal transmission significantly exceeds VP velocity (Vodeneev et al. 2012). The second possible mode of VP propagation is connected with migration of a wound chemical substance from the damaged zone (Ricca 1916; Umrath 1959; Peña-Cortés et al. 1995; Sibaoka 1997; Vodeneev et al. 2012), which is supported by experimental data regarding VP propagation through a solution that connects two parts of a severed stem (Ricca 1916), observed induction of VP-like electrical reactions by wound extracts (Umrath 1959; Sibaoka 1997) and detected similarities between the speed of chemical agent transmission through the stem and the VP propagation velocity (Rhodes et al. 1999; Vodeneev et al. 2012). According to the current concept, the high speed of chemical agent transmission is connected with turbulent diffusion in xylem, which can be accelerated by hydraulic waves (Vodeneev et al. 2012).

Understanding plant VP generation and propagation mechanisms requires experimental investigation as well as simulation. There are a number of models for plant APs (Beilby 1982, 2007; Mummert and Gradmann 1991; Sukhov and Vodeneev 2009; Sukhov et al. 2011); however, mathematical models for VP are lacking. The aim of the present work was to develop a mathematical model for VP generation and propagation in plants. The model employed is based on two hypotheses: (1) VP propagation is connected with wound substance diffusion from the wound site and (2) VP generation is induced by activation of ligand-gated Ca^{2+} channels by a wound substance.

Theory

VP generation has been simulated on the basis of our previously developed model (Sukhov and Vodeneev 2009;

Sukhov et al. 2011) but with modifications (Fig. 1) and includes descriptions of plasma membrane ion transport systems (K^+, Cl^- and Ca^{2+} channels, H^+ and Ca^{2+}-ATPase, $2H^+/Cl^-$ symporter and H^+/K^+ antiporter) and their regulation, ion concentration changes in the cell and extracellular space and buffers in the cytoplasm and apoplast. Inward and outward K^+, Cl^- and Ca^{2+} channels have been described by the Goldman-Hodgkin-Katz equation and equations of open-state probability (p_o) dynamics. H^+ and Ca^{2+}-ATPases have been simulated by a "two-state model" (Hansen et al. 1981; Beilby and Shepherd 2001; Sukhov and Vodeneev 2009), which takes into account two states of a pump, with and without an ion. Velocity constants for transitions between these states depend on ion concentrations as well as the membrane potential (Sukhov and Vodeneev 2009; Sukhov et al. 2011). The H^+/K^+ antiporter and the $2H^+/Cl^-$ symporter are described, using equations, as differences between fluxes directed to the apoplast and to the cytoplasm (Sukhov and Vodeneev 2009; Sukhov et al. 2011).

Changes in ion concentrations in the cytoplasm and apoplast are described on the basis of flux equations, considering ratios between the cell surface and cell volume and between the apoplast and cell volumes (Sukhov and Vodeneev 2009; Sukhov et al. 2011). Buffer capacities of the apoplast (K^+ and H^+) and cytoplasm (H^+) have also been simulated in the model (Sukhov and Vodeneev 2009; Sukhov et al. 2011). An increase in cytoplasmic Ca^{2+} concentration is known to induce Cl^--channel activation (Lewis et al. 1997; Berestovsky and Kataev 2005; Beilby and Shepherd 2006) and H^+-ATPase inactivation (Kinoshita et al. 1995; De Nisi et al. 1999; Vodeneev et al. 2006). The dependence of their activities on calcium ions has been described in the VP model, in accordance with our previous description (Sukhov and Vodeneev 2009; Sukhov et al. 2011).

VP may be connected with the migration of a wound chemical substance from the damage zone (Rhodes et al. 1999; Vodeneev et al. 2012) and with Ca^{2+} influx to the cell (Julien et al. 1991; Vodeneev et al. 2011). Therefore, we suppose that plant plasma membrane contains ligand-gated Ca^{2+} channels activated by the wound substance. The dependence of ligand-gated Ca^{2+}-channel permeability (P_{Ca-LG}) on the wound substance concentration ([WS]) is described by Eq. 1

$$P_{Ca-LG} = \frac{[WS]/WS_0}{K_{Ca-LG}/WS_0 + [WS]/WS_0} P_{Ca-LG}^{max} \qquad (1)$$

where P_{Ca-LG}^{max} is the maximum permeability of ligand-gated Ca^{2+} channels, K_{Ca-LG} is the dissociation constant for the complex of wound substance and ligand-gated Ca^{2+} channel and WS_0 is the initial content of wound substance in the damage zone. It should be noted that we did not take into account the possible role in VP of other Ca^{2+} sources,

Fig. 1 Scheme of a plant cell electrophysiological model (Sukhov et al. 2011, with modifications) and wound substance diffusion. E_m electrical potential of plasma membrane; B_{in}^- and BH_{in} free and H^+-bound proton-buffer molecules in cell, respectively; B_{out}^-, BH_{out} and BK_{out} free, H^+ and K^+-bound buffer molecules in apoplast, respectively; P_{max} maximum permeability; p_o and p_i open state and inactivated state probability of ion channel, respectively; $k_{+o(+i)}$ and $k_{-o(-i)}$ velocity constants of ion channel transitions from closed to open state and vice versa, respectively; o and i open and inactivated states, respectively; E_o ATPase concentration; k_{+1}, k_{-1}, k_{+2} and k_{-2} velocity constants of forward (+) and reverse (−) transitions between two pump states; and V^{Cl} and V^K total velocity constants of $2H^+/Cl^-$ symporter and H^+/K^+ antiporter, respectively
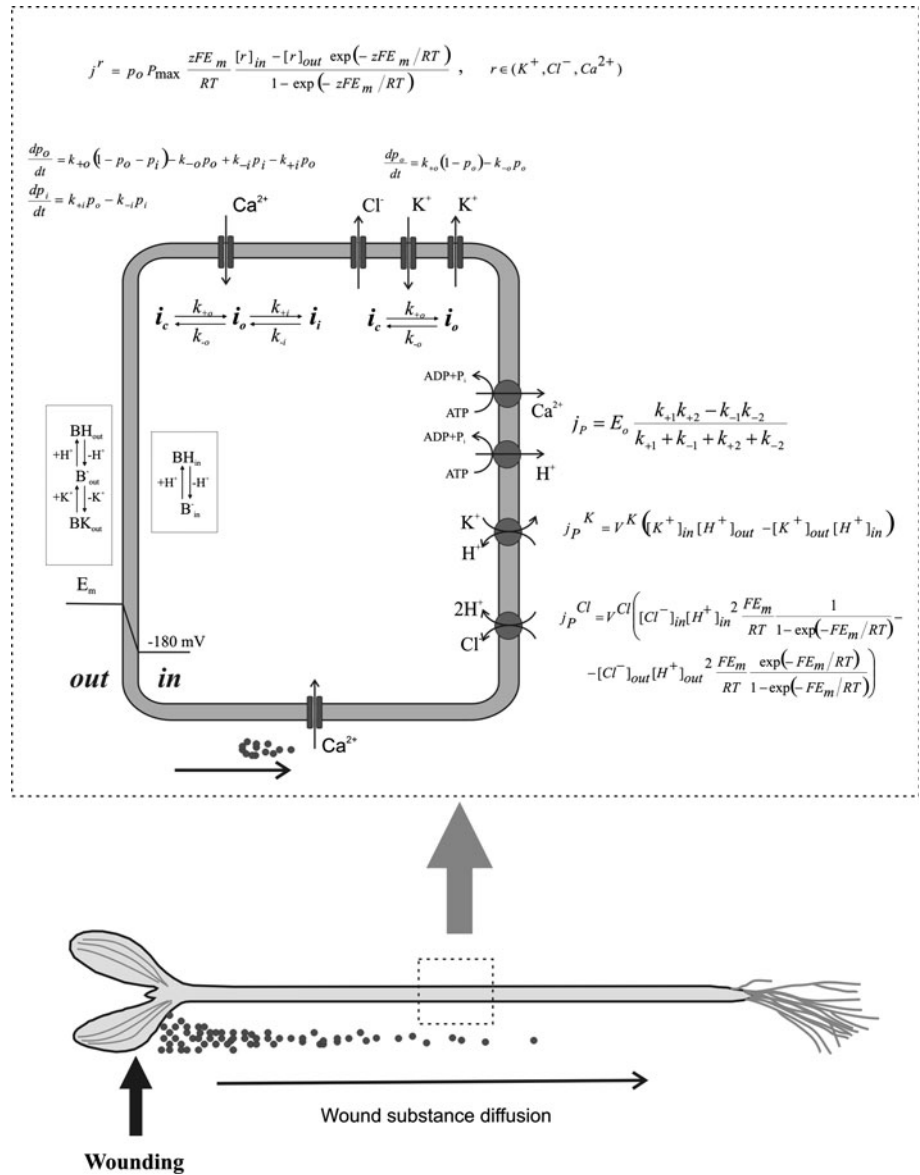
such as vacuoles or endoplasmic reticulum, because their participation in electrical reaction generation in higher plants has been little investigated. However, it is possible that a Ca^{2+} concentration increase has a priority role in VP generation, whereas the specific Ca^{2+} source is rather less important.

The dynamics of wound substance concentration has been described by a one-dimensional diffusion Eq. (2), according to our previous work (Vodeneev et al. 2012)

$$\frac{\partial [WS]}{\partial t} = D \frac{\partial^2 [WS]}{\partial r^2} \qquad (2)$$

where r is the distance from the zone of local damage, t is the time after wounding and D is the coefficient of wound substance diffusion.

The solution of Eq. 2 is Eq. 3 (Codling et al. 2008):

$$\frac{[WS]}{WS_0} = \frac{1}{2\sqrt{\pi Dt}} \exp\left[-\frac{r^2}{4Dt}\right] \qquad (3)$$

The coefficient of wound substance diffusion (D) equals 0.06 cm^2 s^{-1} (Vodeneev et al. 2012). The dissociation-normalized constant for the complex of the wound substance molecule and ligand-gated Ca^{2+} channel ($K_{Ca\text{-}LG}/WS_0$) varies from 0.15 to 3.6 dm^{-1}.

The membrane potential has been described as stationary according to our previous work (Sukhov et al. 2011):

$$E_m = \frac{g_K E_K + g_{Cl} E_{Cl} + g_{Ca} E_{Ca} + g_{PH} E_{PH} + g_{PCa} E_{PCa} + g_{Sy} E_{Sy}}{g_K + g_{Cl} + g_{Ca} + g_{PH} + g_{PCa} + g_{Sy}} \qquad (4)$$

where g_K, g_{Cl}, g_{Ca}, g_{PH}, g_{PCa} and g_{Sy} are electrical conductivities of the K^+, Cl^- and Ca^{2+} channels, H^+ and

Ca²⁺-ATPases and 2H⁺/Cl⁻ symporter, respectively; and $E_{PH} = \frac{\Delta G_{ATP}}{F} + E_H$, $E_{PCa} = \frac{\Delta G_{ATP}}{F} + E_{Ca} - E_H$ and $E_{Sy} = E_{Cl} + 2E_H$ are equilibrium potentials of H⁺ and Ca²⁺-ATPases and 2H⁺/Cl⁻-symporter fluxes, respectively; E_K, E_{Cl}, E_{Ca} and E_H are equilibrium potentials of K⁺, Cl⁻, Ca²⁺ and H⁺, respectively; and $\Delta G_{ATP} = -50$ kJ, the free energy of 1 M ATP. Equation 5 is used for the electrical conductivity description:

$$g_k = \frac{Fj_k}{E_m - E_k} \qquad (5)$$

where j_k and E_k are the flux and equilibrium potential for process k, respectively.

The model equations have been numerically calculated by Euler's method, and values of the majority of the model parameters have been described in previous work (Sukhov and Vodeneev 2009). The maximum permeability of ligand-gated Ca²⁺ channels is 1.5×10^{-7} cm s⁻¹ and the maximum permeability of potential-dependent Ca²⁺ channels is 5×10^{-8} cm s⁻¹. For model verification, experimental data acquired from pumpkin seedling (Vodeneev et al. 2011) have been used. However, in this work, extracellular registration of electrical potential was used, whereas the model simulated intracellular electrical potential changes. Electrical potential dynamics is similar for extracellular and intracellular registration (Zawadzki and Trebacz 1985), but the ratio of the intracellular electrical potential change to the extracellular electrical potential change can differ from 1 (1.5 for pumpkin seedling [Retivin et al. 2001]). For scale compensation, we used a ratio of the model electrical potential scale to the experimental scale equal to 1.5.

Results and Discussion

Figure 2 shows different experimental VP records as well as simulated curves for different distances from the wound site. These VPs were always transient depolarization, but their amplitudes, shapes and durations varied (Fig. 2). We supposed that this variability could have been related to changeability in the initial wound substance concentration. The simulated VP in Fig. 2 revealed that changes in K_{Ca-LG}/WS_0 (a parameter inversely related to wound substance quantity) assured good accordance of the calculated curves with the varying experimental ones. Taking into account this result, we supposed that variation in wound substance quantities was one of the probable causes of VP variability; other causes of VP variability were possible. In particular, variation could be connected with different excitability of cells that take part in the generation of this electrical reaction.

$K_{Ca-LG}/WS_0 = 2$ dm⁻¹ was used in further analyses because simulated curves at some values of this parameter were more typical than with other quantities. Under these conditions, the simulated VP consisted of a long-lasting depolarization wave superimposed with one or a few impulses (Fig. 2b). The amplitude of the long-lasting depolarization decreased with increased distance traveled by this signal, whereas the number of impulses depended on the distance from the wound site in a complex manner.

In spite of high VP variability, the basic rules of VP transformation with increased distance from the wound site have been investigated (Vodeneev et al. 2011, 2012). The dependencies of the long-lasting depolarization amplitude, VP velocity and number of impulses on distances from the wound site are shown in Fig. 3. The similarity between the average experimental and theoretical dependencies of depolarization amplitude and the number of impulses showed that VP can be simulated by the model (Fig. 3a, c). The simulated dependence of the VP velocity was similar to experimental curves in a qualitative manner, whereas values of VP velocities were lower than experimental ones (Fig. 3b). These differences might be explained using diffusion coefficient estimations acquired on wheat seedlings (Vodeneev et al. 2012). The simulated VP velocities were similar to experimental velocities at $D = 0.12$ cm² s⁻¹.

These results supported the suggested schema used as the basis of this model. In particular, it showed wound substance participation in VP propagation and the diffusion mechanism of the substance transmission suggested in our previous work (Vodeneev et al. 2012). Also, according to these results, VP generation was connected with activation of ligand-gated Ca²⁺ channels. However, participation of different ions in VP generation requires further analysis.

The conclusion that calcium influx is possibly an early stage of VP generation is supported by observed decreases in VP amplitude under low extracellular Ca²⁺ concentrations (Julien et al. 1991; Vodeneev et al. 2011). Decreased external calcium ion concentrations (concentration of Ca²⁺ in apoplast equals 10 % of the control) completely suppressed VP generation in the model (Fig. 4), supporting the necessity of Ca²⁺ influx for VP generation. Upon entering the cell, Ca²⁺ ions activate Cl⁻ channels (Lewis et al. 1997; Berestovsky and Kataev 2005; Beilby and Shepherd 2006) as well as inactivate H⁺-ATPase (Smith and Beilby 1983; De Nisi et al. 1999; Vodeneev et al. 2006). However, there were differences between decreases in experimental VP (Fig. 4a) and complete suppression in simulation (Fig. 4b). This might have been connected with the existence of other Ca²⁺ sources, such as vacuoles and endoplasmic reticulum, taking part in the electrical reaction generation; however, for higher plants this question has been little investigated.
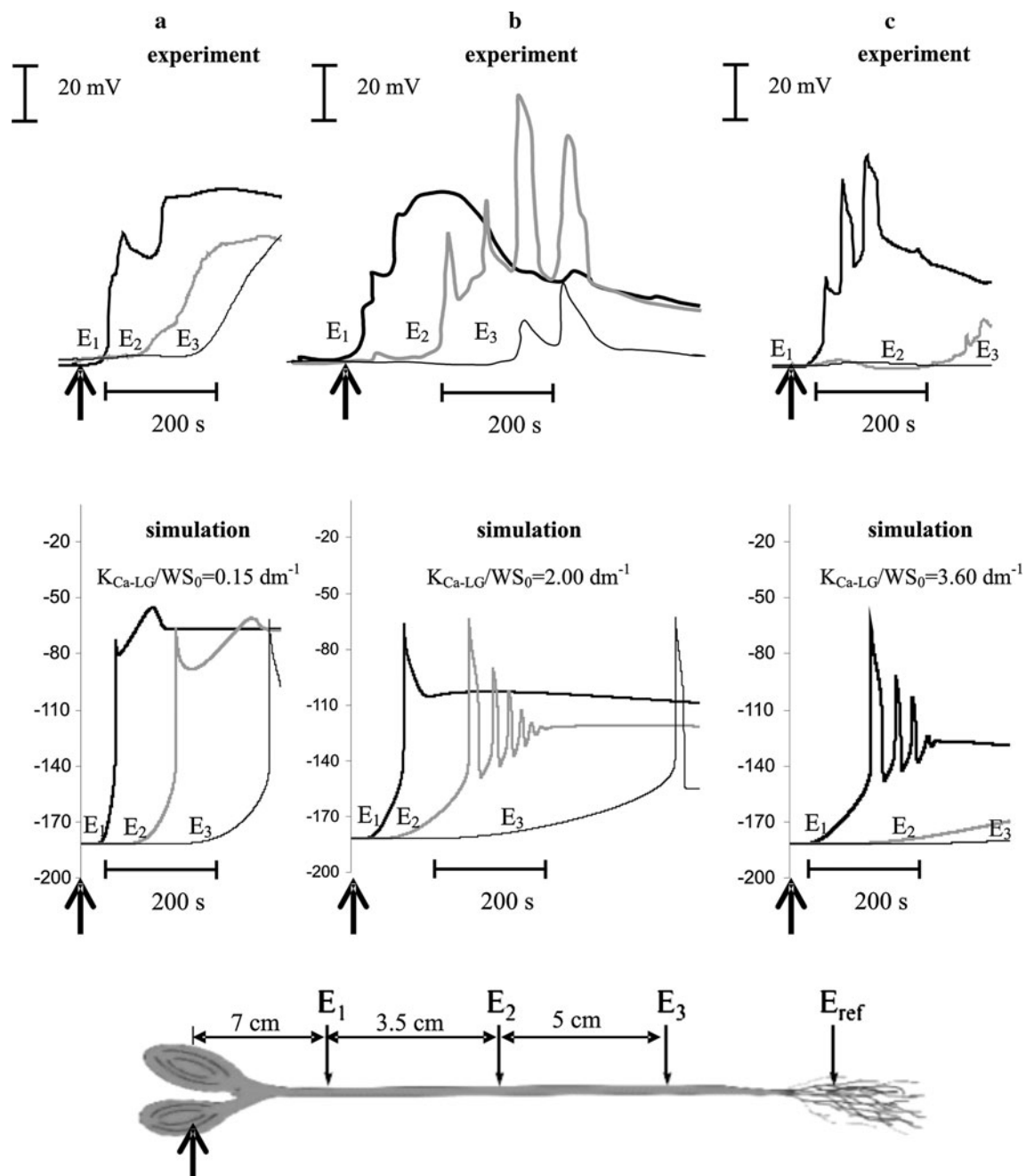
Fig. 2 Records of experimental and simulated variation potentials at different distances from the wounding site. Experimental recordings measured using three extracellular electrodes and a reference (for details, Vodeneev et al. 2011); different variation potential recordings and simulated curves calculated at various values of K_{Ca-LG}/WS_0 in **a**, **b** and **c**. *Arrow* Instant of tip leaf wounding; and distances from wounding site to E_1, E_2 and E_3 equal 7, 10.5 and 15.5 cm, respectively

The hypothesis that VP generation is based on transient H^+-ATPase inactivation is supported by observed decreases in variation potential amplitude under the influence of metabolic inhibitors (Julien et al. 1991; Stahlberg and Cosgrove 1992, 1996). Figure 5 illustrates the VP simulated for low H^+-ATPase activity levels (number of proton pumps per area unit equals 10 % of the control), exhibiting decreased amplitude and depolarization velocity and only one weak impulse. This simulated VP was similar to the experimental electrical reaction that was observed with a metabolic inhibitor, sodium azide (0.5 mM) (Vodeneev et al. 2011). It should be noted that addition of metabolic inhibitors induces membrane depolarization that is not observed in experimental VP recordings because they were measured using extracellular electrodes. This effect was in accordance with previous experimental and theoretical data

Fig. 3 Dependencies of the long-lasting depolarization amplitude **a** the VP velocity **b** and the number of impulses **c** on distances from the wounding site in experiment and simulation. Experimental data used from Vodeneev et al. (2011)
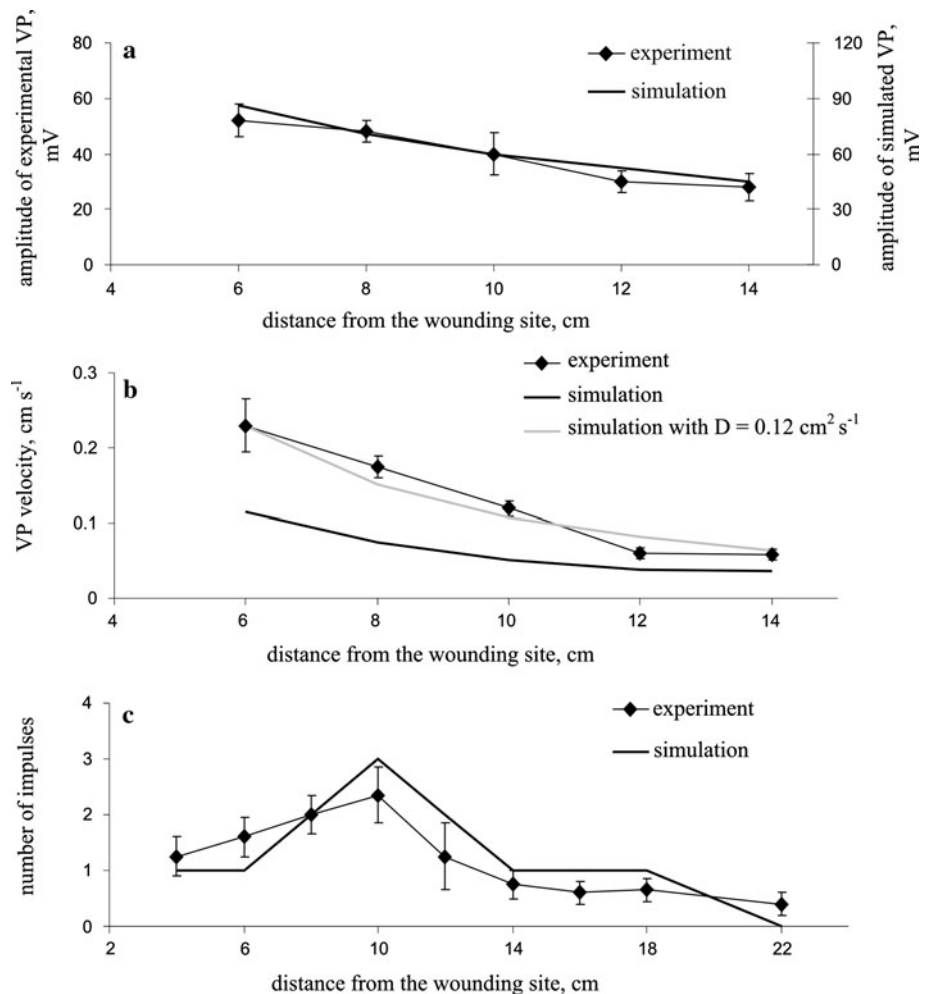
(Vodeneev et al. 2006; Sukhov and Vodeneev 2009). This result could have supported a hypothesis regarding direct H^+-ATPase participation in VP generation, but the influence of proton pump inactivation on the electrical reaction might have been caused by membrane potential decreases and subsequently lower ion gradients (e.g., Ca^{2+} and Cl^- gradients). As a result, analysis of H^+-ATPase participation in VP generation requires further investigation of ion fluxes during VP generation.

The stipulation that Cl^- channel activation might have played a role in VP generation is supported by experimental data (Vodeneev et al. 2011). Figure 6 shows decreased amplitude and depolarization velocity in a simulated VP under low maximum permeability of Cl^- channels (equals 10 % of the control). Also, the VP possessed only one impulse in this case, whereas four impulses were observed under control conditions, which was in good accordance with suppression of VP generation and decreased impulse numbers with the specific anion channel blocker ethacrynic acid (Vodeneev et al. 2011). These

results indicated that Cl^--channel activation was probably one stage of VP generation and that elimination of this stage could have influenced VP amplitude and shape.

Thus, this VP model both qualitatively and quantitatively effectively described the parameters of variation potential (Figs. 2, 3) and qualitatively simulated the influence of inhibitors on this reaction (Figs. 4, 5, 6); consequently, it can be used for further theoretical analysis of VP mechanisms. Simulated VPs have variable shape, including a long-lasting depolarization wave superimposed on a few impulses, with parameters strongly dependent on wound substance concentrations (Fig. 2). Figure 7 shows changes in intracellular Ca^{2+} concentration and the total H^+ and Cl^- fluxes simulated by our model. The dynamics of the H^+ and Cl^- fluxes showed that these fluxes might have induced changes in these ions' concentrations, which were qualitatively similar to experimental values (Vodeneev et al. 2011). Theoretical dynamics of Ca^{2+} concentrations at different distances from the wound site showed that the shape of these dynamics strongly influenced VP

Fig. 6 Experimental a (Vodeneev et al. 2011) and simulated b variation potentials under Cl⁻-channel blockage. Maximum permeability of Cl⁻ channels (E_2 zone) equals 10 % of controls in simulation, and other simulation conditions as in Fig. 2
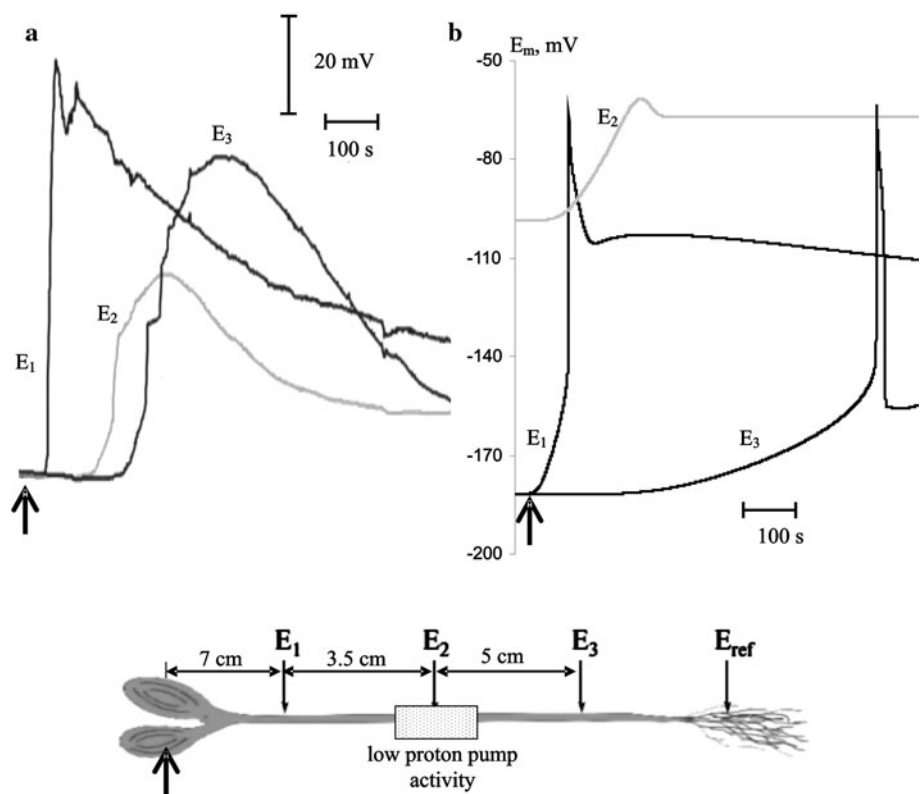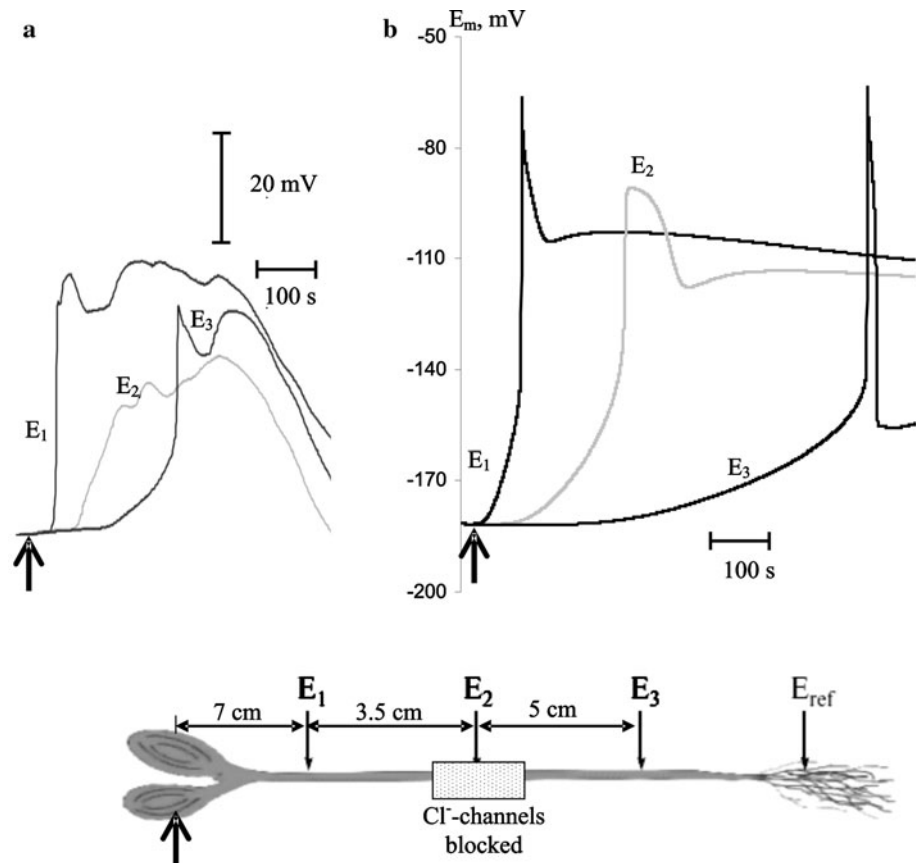
parameters. However, Ca^{2+} concentration increases could have activated Cl^- channels as well as inactivated H^+-ATPase; consequently, the question regarding the contribution of Cl^- and H^+ fluxes to different stages of VP generation becomes important.

Total H^+ and Cl^- fluxes simulated by the model displayed long-lasting depolarization waves that were mainly connected with H^+-ATPase inactivation and proton flux changes, whereas Cl^- flux was only weakly altered (Fig. 7). However, impulses were accompanied by an

essential Cl^- flux as well as H^+ changes. These results supported the hypothesis that the wound substance activated ligand-gated Ca^{2+} channels, which in turn inactivated H^+-ATPase (proton pump inactivation requires Ca^{2+} concentration less than Cl^- channel requires for activation) (Kinoshita et al. 1995; Lewis et al. 1997) and induced a long-lasting depolarization wave. In turn, this wave stimulated potential-dependent Ca^{2+} channels that activated Cl^- channels, raised H^+-ATPase inactivation and induced impulses. The last step of the mechanism was very similar
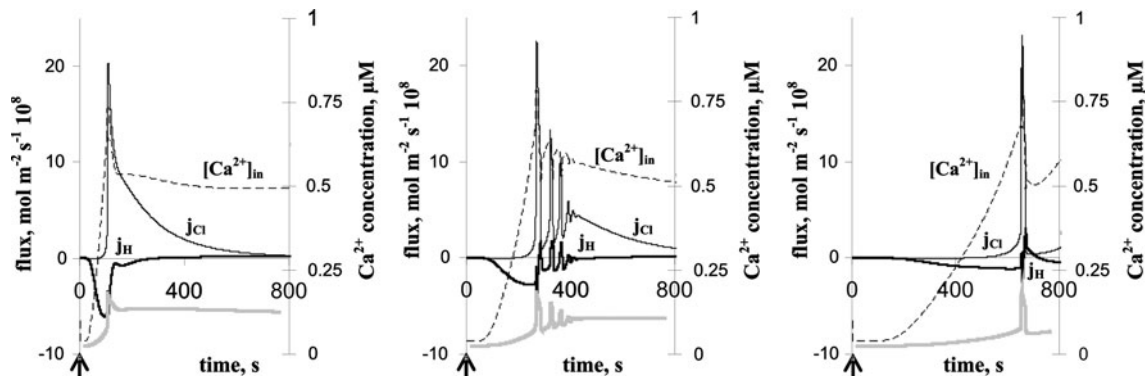

Fig. 7 Simulated Ca^{2+} concentration changes and total H^+ and Cl^- fluxes in variation potential generation at different distances from the wounding site. Distances in a, b and c are 7, 10.5 and 15.5 cm, respectively. Gray line schematically shows changes of E_m (without coordinate axis); − influx, + efflux, arrow instant of tip leaf wounding

to the AP-generation mechanism (Davies 2006; Trebacz et al. 2006; Vodeneev et al. 2006; Felle and Zimmermann 2007; Sukhov and Vodeneev 2009).

Thus, our results illuminated several important points. (1) The model simulated basic properties of VP and could be used for analysis of VP generation and propagation mechanisms. (2) The similarity between the experimental VP and the simulated one supported the following mechanism for variation potential induction: wounding → wound substance formation → turbulent diffusion of wound substance through the stem → activation of ligand-gated plasma membrane Ca^{2+} channels → Ca^{2+} influx → H^+-ATPase inactivation and Cl^--channel activation → generation of the electrical reaction. (3) The model theoretically revealed that long-lasting depolarization was connected with H^+-ATPase inactivation, whereas impulses were caused by Cl^--channel activation, with both processes being Ca^{2+}-dependent.

References

Beilby MJ (1982) Cl^- channels in *Chara*. Philos Trans R Soc Lond B Biol Sci 299:435–445

Beilby MJ (2007) Action potential in charophytes. Int Rev Cytol 257:43–82

Beilby MJ, Shepherd VA (2001) Modeling the current–voltage characteristics of charophyte membranes. II. The effect of salinity on membranes of *Lamprothamnium papulosum*. J Membr Biol 181:77–89

Beilby MJ, Shepherd VA (2006) The characteristics of Ca^{++}-activated Cl^- channels of salt-tolerant charophyte *Lamprothamnium*. Plant Cell Environ 29:764–777

Berestovsky GN, Kataev AA (2005) Voltage-gated calcium and Ca^{2+}-activated chloride channels and Ca^{2+} transients: voltage-clamp studies of perfused and intact cells of *Chara*. Eur Biophys J 34:973–986

Codling EA, Plank MJ, Benhamou S (2008) Random walk models in biology. J R Soc Interface 5:813–834

Davies E (2006) Electrical signals in plants: facts and hypotheses. In: Volkov AG (ed) Plant electrophysiology. Theory and methods, Springer-Verlag, Berlin, pp 407–422

De Nisi P, Dell'Orto M, Pirovano L, Zocchi G (1999) Calcium-dependent phosphorylation regulates the plasma-membrane H^+-ATPase activity of maize (*Zea mays* L.) roots. Planta 209:187–194

Dziubinska H, Filek M, Koscielniak J, Trebacz K (2003) Variation and action potentials evoked by thermal stimuli accompany enhancement of ethylene emission in distant non-stimulated leaves of *Vicia faba* minor seedlings. J Plant Physiol 160:1203–1210

Felle HH, Zimmermann MR (2007) Systemic signaling in barley through action potentials. Planta 226:203–214

Filek M, Koscielniak J (1997) The effect of wounding the roots by high temperature on the respiration rate of the shoot and propagation of electric signal in horse bean seedlings (*Vicia faba* L. minor). Plant Sci 123:39–46

Fisahn J, Herde O, Willmitzer L, Peña-Cortés H (2004) Analysis of the transient increase in cytosolic Ca^{2+} during the action potential of higher plants with high temporal resolution: requirement of Ca^{2+} transients for induction of jasmonic acid biosynthesis and PINII gene expression. Plant Cell Physiol 45:456–459

Fromm J, Lautner S (2007) Electrical signals and their physiological significance in plants. Plant Cell Environ 30:249–257

Grams TEE, Koziolek C, Lautner S, Matyssek R, Fromm J (2007) Distinct roles of electric and hydraulic signals on the reaction of leaf gas exchange upon re-irrigation in *Zea mays* L. Plant Cell Environ 30:79–84

Grams TEE, Lautner S, Felle HH, Matyssek R, Fromm J (2009) Heat-induced electrical signals affect cytoplasmic and apoplastic pH as well as photosynthesis during propagation through the maize leaf. Plant Cell Environ 32:319–326

Hansen U-P, Gradmann D, Sanders D, Slayman CL (1981) Interpretation of current–voltage relationships for "active" ion transport systems: I. Steady-state reaction-kinetic analysis of class-I mechanisms. J Membr Biol 63:165–190

Hlaváčková V, Krchňák P, Nauš J, Novák O, Špundová M, Strnad M (2006) Electrical and chemical signals involved in short-term systemic photosynthetic responses of tobacco plants to local burning. Planta 225:235–244

Julien JL, Desbiez MO, de Jaeger G, Frachisse JM (1991) Characteristics of the wave of depolarization induced by wounding in *Bidens pilosa* L. J Exp Bot 42:131–137

Kinoshita T, Nishimura M, Shimazaki K (1995) Cytosolic concentration of Ca^{2+} regulates the plasma membrane H^+-ATPase in guard cells of fava bean. Plant Cell 7:1333–1342

Koziolek C, Grams TEE, Schreiber U, Matyssek R, Fromm J (2003) Transient knockout of photosynthesis mediated by electrical signals. New Phytol 161:715–722

Lautner S, Grams TEE, Matyssek R, Fromm J (2005) Characteristics of electrical signals in poplar and responses in photosynthesis. Plant Physiol 138:2200–2209

Lewis BD, Karlin-Neumann G, Davis RW, Spalding EP (1997) Ca^{2+}-activated anion channels and membrane depolarizations induced by blue light and cold in *Arabidopsis* seedlings. Plant Physiol 114:1327–1328

Malone M, Stankovic B (1991) Surface potentials and hydraulic signals in wheat leaves following localized wounding by heat. Plant Cell Environ 14:431–436

Mancuso S (1999) Hydraulic and electrical transmission of wound-induced signals in *Vitis vinifera*. Aust J Plant Physiol 26:55–61

Mummert H, Gradmann D (1991) Action potentials in *Acetabularia*: measurement and simulation of voltage-gated fluxes. J Membr Biol 124:265–273

Peña-Cortés H, Fisahn J, Willmitzer L (1995) Signals involved in wound-induced proteinase inhibitor II gene expression in tomato and potato plants. Proc Natl Acad Sci USA 92:4106–4113

Retivin VG, Opritov VA, Lobov SA (2001) A computer electrophysiological investigation of action potential propagation in stem of pumpkin seedling. Vestnik of NNSU [in Russian]. Seriya Biologiya 1:190–197

Rhodes JD, Thain JF, Wildon DC (1999) Evidence for physically distinct systemic signalling pathways in the wounded tomato plant. Ann Bot 84:109–116

Ricca U (1916) Soluzione d'un problema di fisiologia: la propagazione di stimulo nella Mimosa. Nuovo G Bot Ital 23:51–170

Shimmen T (2002) Electrical perception of "death message" in *Chara*: analysis of rapid component and ionic process. Plant Cell Physiol 43:1575–1584

Sibaoka T (1997) Application of leaf extract causes repetitive action potentials in *Biophytum sensitivum*. J Plant Res 110:485–487

Smith JR, Beilby MJ (1983) Inhibition of electrogenic transport associated with the action potential in *Chara*. J Membr Biol 71:131–140

Stahlberg R, Cosgrove DJ (1992) Rapid alteration in growth rate and electric potentials upon stem excision in pea seedlings. Planta 187:523–531

Stahlberg R, Cosgrove DJ (1996) Induction and ionic basis of slow wave potentials in seedlings of *Pisum sativum* L. Planta 200:416–425

Stahlberg R, Cosgrove DJ (1997) The propagation of slow wave potentials in pea epicotyls. Plant Physiol 113:209–217

Stahlberg R, Robert E, Cleland RE, van Volkenburgh E (2006) Slow wave potentials—a propagating electrical signal unique to higher plants. In: Baluška F, Mancuso S, Volkmann D (eds) Communication in plants. Neuronal aspects of plant life, Springer-Verlag, Berlin, pp 291–309

Stanković B, Davies E (1996) Both action potentials and variation potentials induce proteinase inhibitor gene expression in tomato. FEBS Lett 390:275–279

Sukhov V, Vodeneev V (2009) A mathematical model of action potential in cells of vascular plants. J Membr Biol 232:59–67

Sukhov V, Nerush V, Orlova L, Vodeneev V (2011) Simulation of action potential propagation in plants. J Theor Biol 291:47–55

Sukhov V, Orlova L, Mysyagin S, Sinitsina J, Vodeneev V (2012) Analysis of the photosynthetic response induced by variation potential in geranium. Planta 235:703–712

Trebacz K, Dziubinska H, Krol E (2006) Electrical signals in long-distance communication in plants. In: Baluška F, Mancuso S, Volkmann D (eds) communication in plants. Neuronal aspects of plant life. Springer-Verlag, Berlin-Heidelberg, pp 277–290

Umrath K (1959) Der Erregungsvorgang. In: Ruhland W (ed) Handbuch der pflanzenphysiologie, vol 17. Springer, Berlin, pp 24–110

Vodeneev VA, Opritov VA, Pyatygin SS (2006) Reversible changes of extracellular pH during action potential generation in a higher plant *Cucurbita pepo*. Russ J Plant Physiol 53:481–487

Vodeneev VA, Akinchits EK, Orlova LA, Sukhov VS (2011) The role of Ca^{2+}, H^+, and Cl^- ions in generation of variation potential in pumpkin plants. Russ J Plant Physiol 58:974–981

Vodeneev V, Orlova A, Morozova E, Orlova L, Akinchits E, Orlova O, Sukhov V (2012) The mechanism of propagation of variation potentials in wheat leaves. J Plant Physiol 169:949–954

Zawadzki T, Trebacz K (1985) Extra- and intracellular measurements of action potentials in the liverwort *Conocephalum conicum*. Physiol Plant 64:477–481